Published in final edited form as:
Bioorg Med Chem Lett. 2013 February 1; 23(3): 614–619. doi:10.1016/j.bmcl.2012.12.030.

SAR analysis of novel non-peptidic NPBWR1 (GPR7) antagonists

Miguel Guerrero[a], **Mariangela Urbano**[a], **Marie-Therese Schaeffer**[b,d], **Steven Brown**[b,d], **Hugh Rosen**[b,c,d], and **Edward Roberts**[a,b,*]

[a]Department of Chemistry, The Scripps Research Institute, 10550 N. Torrey Pines Rd, La Jolla, CA 92037, United States

[b]Department of Chemical Physiology, The Scripps Research Institute, 10550 N. Torrey Pines Rd, La Jolla, CA 92037, United States

[c]Department of Immunology, The Scripps Research Institute, 10550 N. Torrey Pines Rd, La Jolla, CA 92037, United States

[d]The Scripps Research Institute Molecular Screening Center, 10550 N. Torrey Pines Rd, La Jolla, CA 92037, United States

Abstract

In this Letter we report on the advances in our NPBWR1 antagonist program aimed at optimizing the 5-chloro-2-(3,5-dimethylphenyl)-4-(4-methoxyphenoxy)pyridazin-3(2*H*)-one lead molecule previously obtained from a high-throughput screening (HTS)-derived hit. Synthesis and structure–activity relationships (SAR) studies around the 3,5-dimethylphenyl and 4-methoxyphenyl regions resulted in the identification of a novel series of non-peptidic submicromolar NPBWR1 antagonists based on a 5-chloro-4-(4-alkoxyphenoxy)-2-(benzyl)pyridazin-3(2*H*)-one chemotype. Amongst them, 5-chloro-2-(9*H*-fluoren-9-yl)-4-(4-methoxyphenoxy)pyridazin-3(2*H*)-one **9h** (CYM50769) inhibited NPW activation of NPBWR1 with a submicromolar IC_{50}, and displayed high selectivity against a broad array of off-targets with pharmaceutical relevance. Our medicinal chemistry study provides innovative non-peptidic selective NPBWR1 antagonists that may enable to clarify the biological role and therapeutic utility of the target receptor in the regulation of feeding behavior, pain, stress, and neuroendocrine function.

Keywords

NPBWR1 (GPR7) antagonists; Anorexia; Analgesia; Stress

Neuropeptide W (NPW) and neuropeptide B (NPB) bind and activate two G-protein coupled receptors (GPCRs), namely NPBWR1 (GPR7) and NPBWR2 (GPR8).[1] NPB mRNA is widely distributed throughout the mouse brain and is present in the hippocampus, hypothalamin nucleus, Edinger–Westphal nucleus (EW), locus coerulius, inferior olive and lateral parabrancheal nucleus.[1,2] The expression of NPW is more confined to EW, ventral tegmental area (VTA), periaqueductal gray and dorsal raphe nucleus.[3]

*Corresponding author. Tel.: +1 858 784 7770; fax: +1 858 784 7745. eroberts@scripps.edu (E. Roberts).

Human NPBWR1 was mapped to chromosome 10q11.2-121.1 and NPBWR2 to chromosome 20q13.3. NPBWR1 and NPBWR2 share 64% sequence homology and decrease intracellular cAMP by coupling to the Gi-class of GPCRs.[1,4]

In situ hybridization and tissue binding studies showed that NPBWR1 mRNA is localized in the extended amygdala (central nucleus of the amygdala, bed nucleus of the stria terminalis) and the hypothalamus (suprachiasmatic nucleus, VTA).[1,5]

This neuropeptide system has been hypothesized to play an important role in modulating feeding behavior.[6,1] Intracerebroventricular (i.c.v.) administration of NPW to fasting rats or free-feeding rats before dark phase suppressed food intake and increased both heat production and body temperature.[7] Furthermore, NPBWR1 knockout mice developed adult-onset obesity.[8]

Intrathecal (i.t.) administration of NPW produced analgesic effects in inflammatory pain in the mouse formalin test, but not mechanical or thermal pain.[9] Interestingly, samples taken from patients with inflammatory/immunomediated neuropathies showed a higher expression of NPBWR1 restricted to myelin-forming Schwan cells. Similarly, animal models of acute inflammatory and trauma induced neuropathic pain exhibited an increased myelin-associated expression of NPBWR1, suggesting a central role of this receptor in analgesia.[10]

Remarkably, i.c.v. administration of NPW in the brain reduced seizure activity in mice, suggesting that NPWR1 may be a suitable target for epilepsy.[11]

I.c.v. injection of NPB in male rats elevated prolactin and corticosterone, and decreased growth hormone levels in circulation, suggesting that this peptide may play a physiological role in the neuroendocrine response to stress via the activation of the hypothalamus-pituitary-adrenal axis.[12] NPBWR1 knockout mice showed abnormality in the contextual fear condition test in addition to an increased autonomic and neuroendocrine response to physical stress, suggesting that the impairment of NPBWR1 leads to stress vulnerability.[13] A recent study provided evidence that human genetic differences in NPBWR1 modulate emotional responses to facial expressions, particularly towards angry facial expression; it is speculated that this behavior may be linked to the role of NPBWR1 in modulating fear.[14]

Recently, we reported the identification, design and structure–activity relationships (SAR) of a novel non-peptidic NPBWR1 antagonist chemotype obtained from a high-throughput screening (HTS) of the Molecular Libraries-Small Molecule Repository (MLSMR) library. The 5-chloro-2-(3,5-dimethylphenyl)-4-(4-methoxyphenoxy)pyridazin-3(2*H*)-one **1** (**CYM50557**) was identified as a lead molecule in our NPBWR1 antagonist program (Fig. 1).[15] Its sub-micromolar potency and excellent selectivity against a panel of pharmacologically relevant off-target proteins prompted us to further optimize **1** in an effort to develop an in vivo pharmacological tool to better elucidate the biological role of NPBWR1. In this letter we report on the expansion of the SAR studies around the coil region **a** and the pendant 4-methoxyphenyl moiety **b** (Fig. 1).

Our SAR studies on **1** started by exploring the region **a**. The synthesis of **7a–7al** is depicted in Schemes 1 and 2 and their biological results are listed in Table 1.[16] MOM-protection of N-2 followed by substitution on position 4 of the pyridazinone using the 4-metoxyphenoxide furnished **4**. MOM-deprotection of **4** using boron tribromide (BBr_3) yielded the key intermediate **5**. Alkylation of **5** with a series of electronically and structurally diverse alkyl halides **6a-6ag** and **6aj–6al** furnished the final compounds **7a–7ag** and **7aj–7al** (Scheme 1). Compound **7ag** was reduced with lithium borohydride ($LiBH_4$) to give **7ah** which was transformed to **7ai** using acetyl chloride (Scheme 2).

The cyclopentyl analog **7a** was ~14-fold less potent than **1**. Interestingly, the benzyl derivative **7b** was only ~3-fold less potent than **1** indicating that the insertion of a methylene between the aromatic nucleus and the pyridazinone is tolerated in region **a** of the chemotype. The attachment of a methyl group in the *ortho* position of the phenyl ring (**7c**) led to twofold increase in potency compared to the unsubstituted **7b**, whereas a ~2-fold decrease of potency was observed for the *meta*- and *para*-methyl substituted analogs (**7d, 7e**). Similarly, the 2-trifluoromethyl analog **7f** was twofold more potent than **7b**, whereas a mild decrease of potency was observed for the 3-trifluoromethyl **7g** and 4-trifluoromethyl **7h** analogs. Interestingly, an increase of potency versus the mono-substituted counterparts was observed when a second methyl group was added in the *ortho, meta* or *para* position of **7c, 7d, 7e**. Indeed, the 2,6-dimethyl **7i** and 3,5-dimethyl **7j** analogs were ~1.5- and ~3.4-fold more potent than **7c** and **7d**, respectively, while the 3,4-dimethyl analog **7k** was ~2- and ~3-fold more potent than **7d** and **7e**, respectively. Furthermore, the 4-methoxy **7l**, 4-phenyl **7m** and 4-isopropyl **7n** analogs were less potent than **7b** by ~5-, ~12- and ~13-fold, respectively, thus showing that installing electron-donating, aromatic or alkylic groups in *para* position is detrimental for the potency. The potency was impacted to a lesser extent when a chlorine was inserted in *para* position, with **7o** being slightly more potent than **7b**. Further exploring the *ortho* position showed that increasing the size from a methyl (**7c**) to an ethyl group (**7p**) led to a small increase in potency, while the isopropyl derivative **7q** was slightly less potent than **7p**. The 2-methoxy analog **7r** was nearly equipotent to the isopropyl analog **7q**. Interestingly, the methyl ester **7s** and cyano **7t** derivatives were 3- to 4-fold less potent than **7c**. Notably, the biphenyl derivative **7u** was only 1.5-fold less potent than **7c**, while the pyrazole **7v** was slightly more potent than **7c** and **7p**. Taken together this data suggests that both steric and electronic factors in the *ortho* position modulate the potency. Next, we explored the installation of bicyclic and tricyclic aromatic systems in the region **a**. The anthracene **7w** was ~2-fold more potent than **7b** and slightly less potent than the pyrazole **7v**. Remarkably, the naphtalen-2-yl analog **7x** was ~4-fold less potent than **7c**, while the naphtalen-1-yl **7y** (**CYM50719**) was ~3-fold more potent than **7c**. Based on these results we explored the SAR around the naphthalen-1-yl moiety. Introducing an additional methylene spacer between the pyridazinone and the naphthalenyl ring (**7z**) led to 30-fold loss of potency. Installing a methyl in position 2 (**7ab**) led to a small decrease in potency compared to **7y**, and a 2- to 3-fold loss of potency was observed for the 2-methoxy analog **7ac**. The installation of a fluorine (**7aa**), methyl (**7ae**) and bromine (**7ad**) at position 4 led to ~3-, ~3- and ~14-fold loss in potency, respectively, confirming that substitutions in this position are not tolerated. Interestingly, the quinoline **7af** was ~24-fold less potent than the naphthalene **7y** indicating that the basic atom in this position is detrimental for the potency. Next, a series of analogs with disubstituted benzylic position was explored keeping, first, the naphtalen-1-yl as the constant moiety. Interestingly, the ethyl ester **7ag** was ~3-fold less potent than the non-substituted **7y**. Surprisingly, the acetate **7ai** and the primary alcohol **7ah** were ~83- and ~18-fold less potent than **7y**, respectively. Interestingly, the methyl **7aj** and phenyl **7ak** substituted analogs were ~13- and ~128-fold less potent than **7y**. Additionally, the phenyl ketone **7al** was slightly more potent than the non-substituted **7b**. This data showed that steric interactions in this portion of the molecule are important for the potency, and indicated only a minor decrease of the potency when the second substituent contains a carbonyl group immediately attached to the benzylic carbon (**7ag, 7al**). We speculated that the partial ketoenol tautomerization could positively impact the potency by forcing the benzylic substituents into a quasi-planar conformation. Based on this working hypothesis, we synthesized planar or planar-like tricyclic structures (**9a–9h**). The synthesis of these derivatives is depicted in Schemes 3 and 4. Furthermore, the biphenyl system was opened and a carbonyl group was inserted to obtain the quasi-planar ketone **9j** and the amide **9k**. Additionally, the bicyclic amide **9i** was studied. The synthesis of **9i–9k** is depicted in Scheme 5. Coupling of pyridazinone **5** with a series of tricyclic systems **8a–8e** using Ullman

conditions led to the products **9a–9e** (Scheme 3). Alkylation of intermediate **5** with benzylchlorides **10a–10c** using sodium hydride as the base led to the formation of **9f–9h**. Alkylation of **5** with the α-halo carbonyl **11, 12a** and **12b** using potassium carbonate as the base furnished **9i–9k**. The biological data of **9a–9k** is reported in Table 2.[16]

Remarkably, the dibenzoxazepines **9a** and **9b** were slightly more potent than the ketone **7at**. Surprisingly, the dibenzothiazepine **9c** was >50-fold less potent than **9b**. Interestingly the benzopyridoxazepine **9d** was less than twofold less potent than the carba-analog **9a**, showing that the insertion of a basic center in this series was tolerated. When the oxygen from **9b** was exchanged for a carbonyl group (**9e**) the potency decreased by ~4-fold. Removing the imine from the tricyclic system led to the tricyclic compounds **9f–9h**. Remarkably, the fluorene **9h** (**CYM50769**) was slightly more potent than the naphtalen-1-yl derivative **7y**. Increasing the middle-ring size from 5 to 7 members (**9g**) led to 150-fold loss in potency. The xanthene **9f** was ~26-fold less potent than **9h**. Interestingly, the elongated bicyclic analog **9i** was only ~6-fold less potent than the fluorene **9h** indicating that is possible to increase the distance between the pyridazinone and the aromatic rings without major decrement in the potency. Furthermore, the biphenyl ketone **9j** was nearly equipotent to the tricyclic system **9b** and slightly more potent than **7at**. Interestingly, the biphenylamide **9k** was slightly more potent than the carba-analog **9j**.

Next, we explored the region **b** while selecting three moieties from the region **a**. The synthesis of **15a–15w** is depicted in Scheme 6. The results are listed in Table 3. [16] Alkylation of pyridazinone **2** with chlorides **6c, 6ac** and **10c** using potassium carbonate yielded the intermediates **13a–13c**. Substitution with a series of phenols in position 4 of pyridazinones **13a–13c** using sodium hydride as the base yielded the final products **15c–15w** and the intermediates **16a, 16b** which were deprotected to the primary alcohols **15a, 15b** using tetrabutyl ammonium fluoride (TBAF).

First, we attached solubility-enhancing groups in this portion of the molecule. Interestingly the 2-methylbenzyl primary alcohol **15a** was only ~2-fold less potent than the 4-methoxy counterpart **7c**, while the naphthalenyl alcohol **15b** was ~31-fold less potent than **7y** indicating that the 2-methylbenzyl and naphthalenyl series differ in their SAR. We further explored the region **b** while keeping the naphthalene in the region **a**. Adding a fluorine in position 2 (**15c**) or 3 (**15d**) of the phenyl ring, decreased the potency by ~4- and ~2-fold, respectively compared to **7y**, indicating that changing the dipolar moment in the phenyl ring influences negatively the antagonist activity. Next, the SAR at position 4 was explored. The ethoxy analog **15e** (**CYM50775**) was slightly more potent than **7y**. Conversely, the *n*-propoxy **15f** and isopropoxy **15i** were ~8- and ~4-fold less potent than **7y**, respectively, suggesting that steric factors modulate the potency. Remarkably, the ethyl **15g** was less than twofold less potent than **7y** indicating that the hydrogen bond acceptor capability in this position is not fundamental for the functional activity. Furthermore, the trifluoromethoxy **15h** was ~39-fold less potent than **7y**, and a dramatic loss of potency was observed for the methyl ester **15j**, while changing the oxygen of **7y** for sulfur (**15k**) decreased the potency only by threefold. Next, we explored the position 3 of the phenyl ring. The methoxy **15l**, ethoxy **15m** and ethyl **15n** analogs were ~4-, 10- and 34-fold less potent than **7y, 15e** and **15g** respectively. Remarkably, the 3,4-dimethoxy **15o** and 3,4,5-trimethoxy **15p** were 2- and ~13-fold less potent than **7y** suggesting that the negative effect of polisubtitution on the aromatic ring is additive. Since the methoxy on position 3 of **15o** was tolerated, we speculated that bicyclic systems may improve the potency. However, the benzofuran **15q** was ~3-fold less potent than **15o**, while the dihydrobenzofurane **15r** was less than ~2-fold less potent than **15o** and ~2-fold more potent than the indene **15s**. Different SAR was observed within the fluoren-9-yl series. The ethoxy **15t** and ethyl **15u** analogs were

equipotent and twofold less potent than **9h**, while a dramatic decrease in potency was observed for the 4-trifluoromethoxy **15v** and 4-propoxy **15w**.

Amongst the synthesized compounds, **9h** (**CYM50769**) was selected for further characterization.[17] The solubility of **9h** in a phosphate buffered saline (PBS) at pH 7.4 is 0.17 μM. The compound is non-cytotoxic to U2OS cells at 20 μM and chemically stable in PBS at pH 7.4 with half-life higher than 48 h. The selectivity profile was investigated against the Ricerca panel of off-target proteins including GPCRs, enzymes, transporters and ion channels at a concentration of 30 μM. Remarkably, out of 35 tested targets only CYP450 1A2, 5-HT_{2B} and CYP450 2C19 showed 67%, 63% and 51% inhibition, respectively.

In summary, we have reported the synthesis and SAR studies around the coil and 4-methoxyphenyl regions (**a, b**) of novel non-peptidic NPBWR1 antagonists based on a 5-chloro-4-(4-alkoxyphenoxy)-2-(benzyl)pyridazin-3(2*H*)-one chemotype. Small changes in region **b** had a negative impact on the potency, while the region **a** was found to interact with a liphophilic pocket that can accommodate a great variety of bulky quasi-planar substituents. Our studies resulted in the identification of a novel series of submicromolar NPBWR1 antagonists including **7y** (**CYM50719**), **9h** (**CYM50769**) and **15e** (**CYM50775**) endowed with greater potency than our previously reported lead **1**. Amongst them, **9h** was further profiled and found to be highly selective against a broad array of off-targets with pharmaceutical relevance, making this compound suitable for further development. Our medicinal chemistry advances around this chemotype will be communicated in due course.

Acknowledgments

This work was supported by the National Institute of Health Molecular Library Probe Production Center Grant U54 MH084512 (Peter Hodder, Hugh Rosen).

References and notes

1. Tanaka H, Yoshida T, Miyamoto N, Motoike T, Kurosu H, Shibata K, Yamanaka A, Williams SC, Richardson JA, Tsujino N, Garry MG, Lerner MR, King DS, O'Dowd BF, Sakurai T, Yanagisawa M. Proc Natl Acad Sci U S A. 2003; 100:6251. [PubMed: 12719537]
2. Jackson VR, Lin SH, Wang Z, Nothacker HP, Civelli O. J Comp Neurol. 2006; 497:367. [PubMed: 16736466]
3. Kitamura Y, Tanaka H, Motoike T, Ishii M, Williams SC, Yanagisawa M, Sakurai T. Brain Res. 2006; 1093:123. [PubMed: 16697979]
4. O'Dowd BF, Scheideler MA, Nguyen T, Cheng R, Rasmussen JS, Marchese A, Zastawny R, Heng HH, Tsui L, Shi X, Asa S, Puy L, George SR. Genomics. 1995; 28:84. [PubMed: 7590751]
5. Lee DN, Nguyen T, Porter CA, Cheng R, George SR, O'Dowd BF. Brain Res Mol Brain Res. 1999; 71:96. [PubMed: 10407191]
6. Shimomura Y, Harada M, Goto M, Sugo T, Matsumoto Y, Abe M, Watanabe T, Asami T, Kitada C, Mori M, Onda H, Fujino M. J Biol Chem. 2002; 277:35826. [PubMed: 12130646]
7. Mondal MS, Yamaguchi H, Date Y, Shimbara T, Toshinai K, Shimomura Y, Mori M, Nakazato M. Endocrinology. 2003; 144:4729. [PubMed: 12959997]
8. Ishii M, Fei H, Friedman JM. Proc Natl Acad Sci U S A. 2003; 100:10540. [PubMed: 12925742]
9. Yamamoto T, Saito O, Shono K, Tanabe S. Brain Res. 2005; 1045:97. [PubMed: 15910767]
10. Zaratin PF, Quattrini A, Previtali SC, Comi G, Hervieu G, Scheideler MA. Mol Cell Neurosci. 2005; 28:55. [PubMed: 15607941]
11. Green BR, Smith M, White KL, White HS, Bulaj G. ACS Chem Neurosci. 2011; 2:51. [PubMed: 22826747]

12. Samson WK, Baker JR, Samson CK, Samson HW, Taylor MM. J Neuroendocrinol. 2004; 16:842. [PubMed: 15500544]

13. Nagata-Kuroiwa R, Furutani N, Hara J, Hondo M, Ishii M, Abe T, Mieda M, Tsujino N, Motoike T, Yanagawa Y, Kuwaki T, Yamamoto M, Yanagisawa M, Sakurai T. PLoS ONE. 2011; 6:e16972. [PubMed: 21390312]

14. Watanabe N, Wada M, Irukayama-Tomobe Y, Ogata Y, Tsujino N, Suzuki M, Furutani N, Sakurai T, Yamamoto M. PLoS ONE. 2012; 7:e35390. [PubMed: 22545105]

15. Urbano, M.; Guerrero, M.; Zhao, J.; Velaparthi, S.; Saldanha, SA.; Chase, P.; Civelli, O.; Hodder, P.; Schaeffer, M.; Brown, S.; Rosen, H.; Roberts, E. Bioorg Med Chem Lett. 2000. http://dx.doi.org/10.1016/j.bmcl.2012.09.074

16. The biological inhibition assay employed a chimeric cell line that forces the receptor to use Gqi3; therefore the assay readout was calcium release. HEK cells stably co-transfected with the human NPBWR1 and Gqi3 (hGPR7 HEK293T/Gqi3 cell line) were used for this study. Cells were plated at 10,000 cells/well of a 384 well plate in 25 μL media and incubated overnight. Next, 25 μL of Fluo8 NW (ABD Bioquest) was added to all wells and the assay plate incubated for 50 min at 37 °C, 5% CO_2 and 95% relative humidity. Test compounds were added and the assay plate was incubated for 15 min at room temperature. The assay was started by performing a basal read of fluorescence (495 nm excitation and 515 nm emission) for 15 s on the FLIPR Flexstation II 384 (Molecular Devices). Next, 5.5 μl of GPR7 agonist (20 nM final concentration = EC_{80}) in FLIPR Buffer (HBSS/20 mM Hepes/0.1% BSA) or FLIPR Buffer alone were dispensed to the appropriate wells. Then a real time fluorescence measurement was immediately performed for the remaining 45 s of the assay. Tested compounds were assayed in triplicate in an 8-point 1:3 dilution series starting at a nominal concentration of 20 μM. For each test compound, percent inhibition was plotted against the log of the compound concentration. A three parameter equation describing a sigmoidal dose–response curve was then fitted using GraphPad Prism (GraphPad Software Inc) normalized from 0 to 100 for each assay. In cases where the highest concentration tested (i.e. 20 μM) did not result in greater than 50% activation, the IC_{50} was determined manually as greater than 20 μM.

17. http://pubchem.ncbi.nlm.nih.gov/assay/assay.cgi?aid=1880

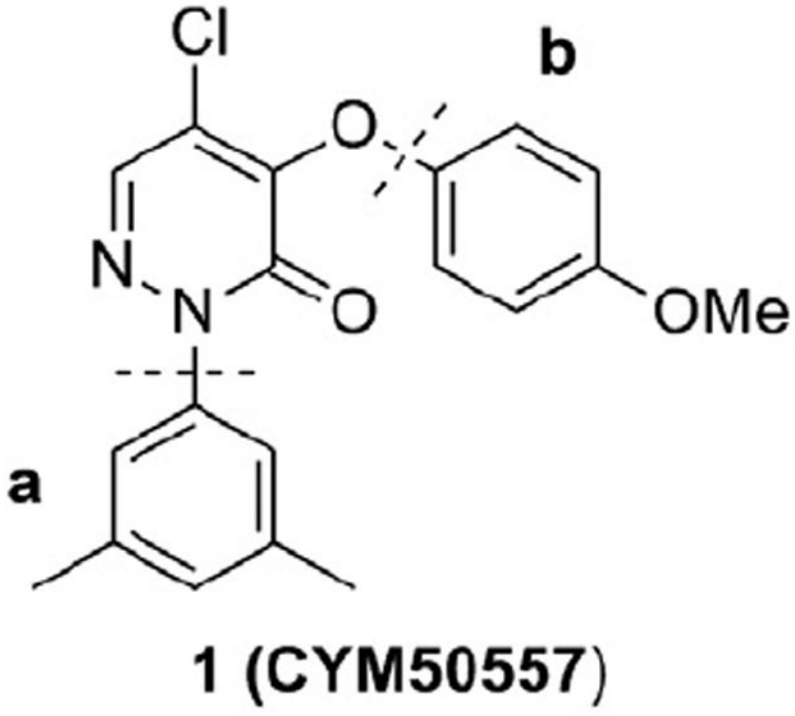

Figure 1.
NPBWR1 lead molecule.
NPBWR1, IC_{50} (μM) = 0.27

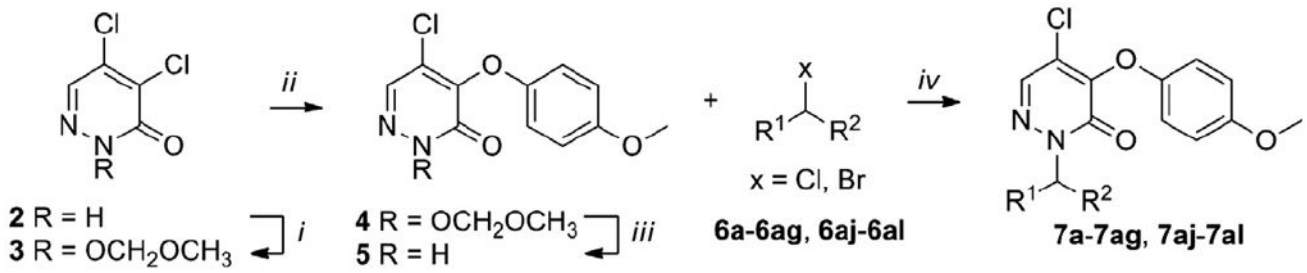

Scheme 1.

Synthesis of **7a–7ag, 7aj–7al**.

Reagents and conditions: (i) **2** (1 equiv.), MOMCl (1.2 equiv.), DMAP (0.1 equiv.), DIPEA (1.4 equiv.) CH_2Cl_2, 0°C to rt, overnight, 85%; (ii) **3** (1 equiv.), 4-methoxyphenol (1.1 equiv.), NaH (1.1 equiv.), 1,4-dioxane, 15°C to rt, overnight, 65%; (iii) **4** (1 equiv.), BBr_3 (1.1 equiv.), CH_2Cl_2, -78°C to rt, 1h, 93%; (iv) **5** (1 equiv.), **6a-6ag**, **6aj-6al** (1.2 equiv.), K_2CO_3 (1.5 equiv.), DMF, rt, overnigt, 40-95%.

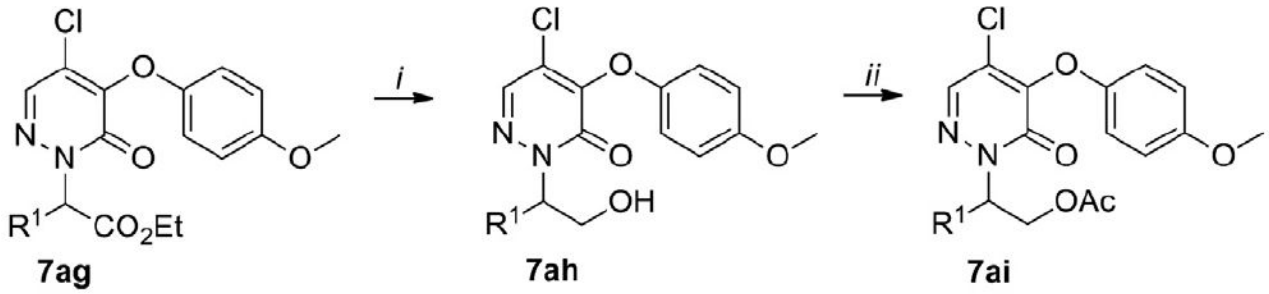

Scheme 2.

Synthesis of **7ah–7ai**.

Reagents and conditions: (i) **7ag** (1 equiv.), $LiBH_4$ (1 equiv.), THF, reflux, 2h, 28%; (ii) **7ah** (1 equiv.), AcCl (1 equiv.), CH_2Cl_2, rt, 2h, 95%.

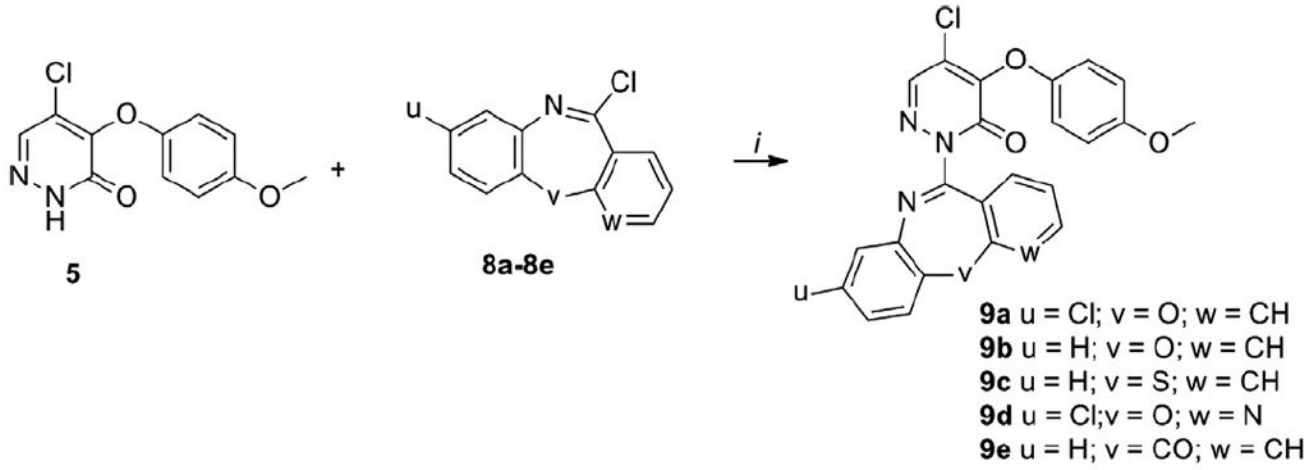

Scheme 3.
Synthesis of **9a–9e**.
Reagents and conditions: (i) **5** (1 equiv.), **8a-8e** (1.3 equiv.), CuI (0.1 equiv.), K_2CO_3 (1.2 equiv.), DMF, 110°C, 8h, 30-65%.

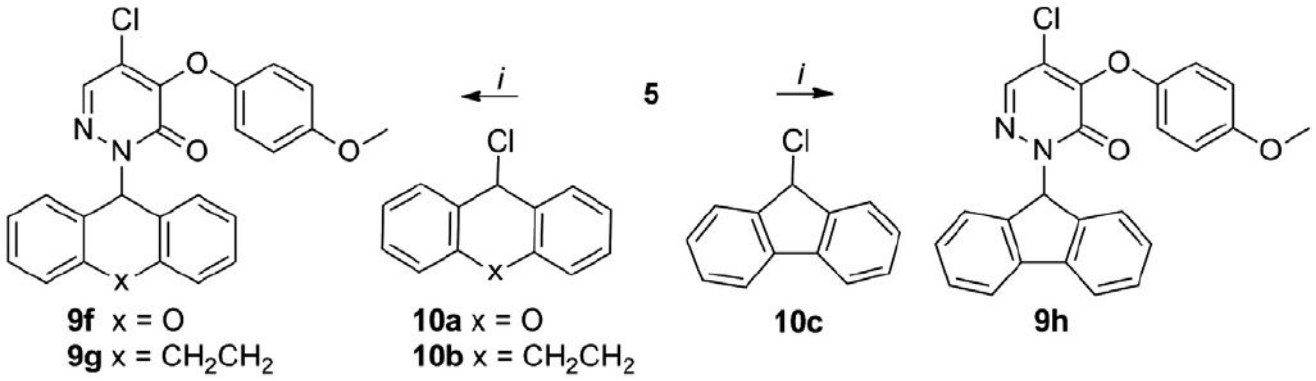

Scheme 4.

Synthesis of **9f–9h**.

Reagents and conditions: (i) **5** (1 equiv.), **10a, 10b, 10c** (1.4 equiv.), NaH (1.1 equiv.), DMF, 0°C to rt, 30-50%.

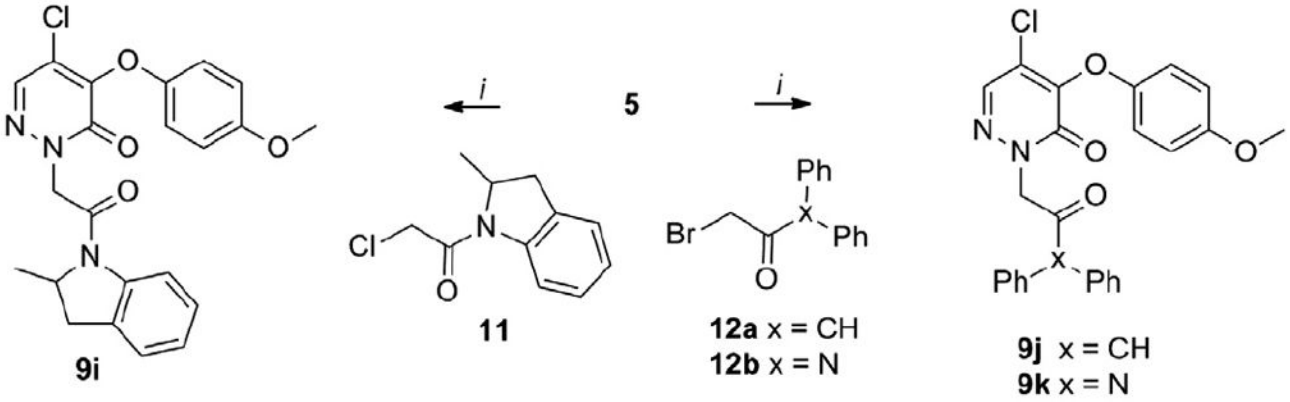

Scheme 5.

Synthesis of **9i–9k**.

Reagents and conditions: (i) **5** (1 equiv.), **11, 12a, 12b** (1.2 equiv.), K_2CO_3 (1.5 equiv.), DMF, rt, overnight, 40-95%.

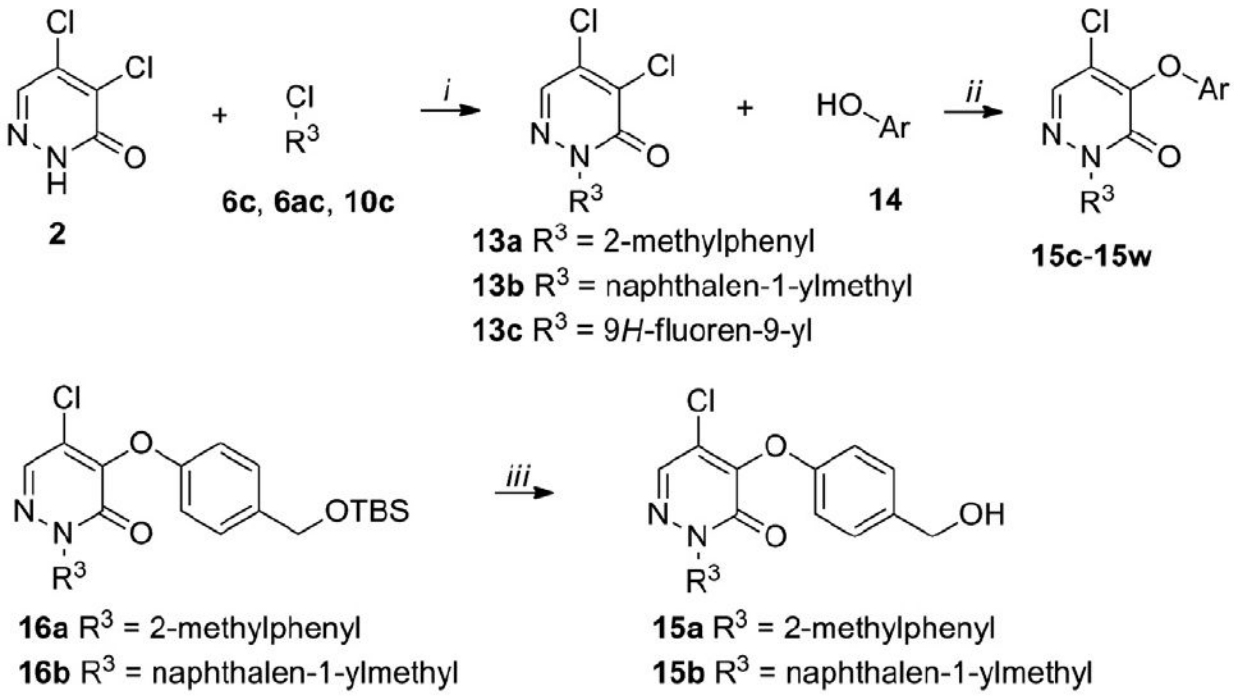

Scheme 6.

Synthesis of **15a–15w**.

Reagents and conditions: (i) **2** (1 equiv.), **6c, 6ac, 10c** (1.2 equiv.), K_2CO_3 (1.5 equiv.), DMF, rt, overnight, 40-95%; (ii) **13a-c** (1 equiv.), **14** (1.1 equiv.), NaH (1.1 equiv.), 1,4-dioxane, 15°C to rt, overnight, 30-70%; (iii) **16a,b** (1 equiv.), TBAF (2 equiv.), THF, 0°C, 1h, 60-90%.

Table 1

NPBWR1 antagonist activity of compounds **7a–7al** (IC_{50} μM)

Compound	R^1	R^2	IC_{50}
7a	Cyclopentyl	H	3.70
7b	Phenyl	H	0.78
7c	2-Methylphenyl	H	0.37
7d	3-Methylphenyl	H	1.40
7e	4-Methylphenyl	H	1.70
7f	2-Trifluoromethylphenyl	H	0.37
7g	3-Trifluoromethylphenyl	H	1.80
7h	4-Trifluoromethylphenyl	H	1.00
7i	2,6-Dimethylphenyl	H	0.24
7j	3,5-Dimethylphenyl	H	0.41
7k	3,4-Dimethylphenyl	H	0.61
7l	4-Methoxyphenyl	H	3.80
7m	4-Phenylphenyl	H	9.40
7n	4-Isopropylphenyl	H	10.0
7o	4-Chlorophenyl	H	0.59
7p	2-Ethylphenyl	H	0.26
7q	2-Isopropylphenyl	H	0.64
7r	2-Methoxyphenyl	H	0.67
7s	2-(Methoxycarbonyl)phenyl	H	1.20
7t	2-Cyanophenyl	H	1.40
7u	(1,1′-Biphenyl)-2-yl	H	0.54
7v	2-(Pyrazol-1-yl)phenyl	H	0.22
7w	Anthracen-9-yl	H	0.32
7x	Naphtalen-2-yl	H	1.50
7y	Naphtalen-1-yl	H	0.14
7z	Naphthalen-1-ylmethyl	H	4.20
7aa	4-Fluoronaphtalen-1-yl	H	0.36
7ab	2-Methylnaphtalen-1-yl	H	0.22
7ac	2-Methoxynaphtalen-1-yl	H	0.35
7ad	4-Bromonaphtalen-1-yl	H	2.00
7ae	4-Methylnaphtalen-1-yl	H	0.37
7af	Quinolin-5-yl	H	3.40
7ag	Naphtalen-1-yl	CO_2Et	0.45
7ah	Naphtalen-1-yl	CH_2OH	2.50
7ai	Naphtalen-1-yl	CH_2OAc	11.60
7aj	Naphtalen-1-yl	Me	1.90
7ak	Naphtalen-1-yl	Phenyl	18.00
7al	Phenyl	COPh	0.58

[a]Data are reported as mean of $n = 3$ determinations.

Table 2

NPBWR1 antagonist activity of compounds **9a–9k** (IC_{50} μM)

Compound	IC_{50} (μM)[a]
9a	0.37
9b	0.49
9c	>25
9d	0.53
9e	2.20
9f	3.10
9g	18.00
9h	0.12
9i	0.78
9j	0.43
9k	0.28

[a] Data are reported as mean of $n = 3$ determinations.

Table 3

NPBWR1 antagonist activity of compounds **15a–15w**

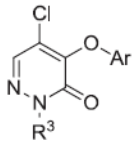

Compound	R^3	Ar	IC_{50}[a] (μM)
15a	2-Methylbenzyl	4-(Hydroxymethyl)phenyl	0.73
15b	Naphthalen-1-ylmethyl	4-(Hydroxymethyl)phenyl	4.40
15c	Naphthalen-1-ylmethyl	2-Flouro-4-methoxyphenyl	0.64
15d	Naphthalen-1-ylmethyl	3-Fluoro-4-methoxyphenyl	0.36
15e	Naphthalen-1-ylmethyl	4-Ethoxyphenyl	0.10
15f	Naphthalen-1-ylmethyl	4-Propoxyphenyl	1.10
15g	Naphthalen-1-ylmethyl	4-Ethylphenyl	0.25
15h	Naphthalen-1-ylmethyl	4-Trifluoromethoxyphenyl	5.50
15i	Naphthalen-1-ylmethyl	4-Isopropoxyphenyl	0.53
15j	Naphthalen-1-ylmethyl	4-(Methoxycarbonyl)phenyl	>20.00
15k	Naphthalen-1-ylmethyl	4-(Methylthio)phenyl	0.43
15l	Naphthalen-1-ylmethyl	3-Methoxyphenyl	0.61
15m	Naphthalen-1-ylmethyl	3-Ethoxyphenyl	0.98
15n	Naphthalen-1-ylmethyl	3-Ethylphenyl	8.50
15o	Naphthalen-1-ylmethyl	3,4-Dimethoxyphenyl	0.29
15p	Naphthalen-1-ylmethyl	3,4,5-Trimethoxyphenyl	1.80
15q	Naphthalen-1-ylmethyl	Benzofuran-5-yl	0.82
15r	Naphthalen-1-ylmethyl	2,3-Dihydrobenzofuran-5-yl	0.43
15s	Naphthalen-1-ylmethyl	2,3-Dihydro-1*H*-inden-5-yl	0.83
15t	9*H*-Fluoren-9-yl	4-Ethoxyphenyl	0.25
15u	9*H*-Fluoren-9-yl	4-Ethylphenyl	0.24
15v	9*H*-Fluoren-9-yl	4-Trifluoromethoxyphenyl	>20.00
15w	9*H*-Fluoren-9-yl	4-Propoxyphenyl	>20.00

[a]Data are reported as mean of $n = 3$ determinations.